

Emerging applications of nanocatalysts synthesized by flame aerosol processes

Yuan Sheng¹, Markus Kraft^{1,2}, Rong Xu¹

released: 6 February 2018

¹ School of Chemical and Biomedical Engineering
Nanyang Technological University
62 Nanyang Drive
637459
Singapore
Email: rxu@ntu.edu.sg

² Department of Chemical Engineering and Biotechnology
University of Cambridge
West Cambridge Site
Philippa Fawcett Drive
Cambridge, CB3 0AS
United Kingdom
E-mail: mk306@cam.ac.uk

Preprint No. 196



Keywords: nanomaterial, catalysis, flame aerosol synthesis, flame spray pyrolysis, energy, environment

Edited by

Computational Modelling Group
Department of Chemical Engineering and Biotechnology
University of Cambridge
West Cambridge Site
Philippa Fawcett Drive
Cambridge CB3 0AS
United Kingdom

Fax: + 44 (0)1223 334796

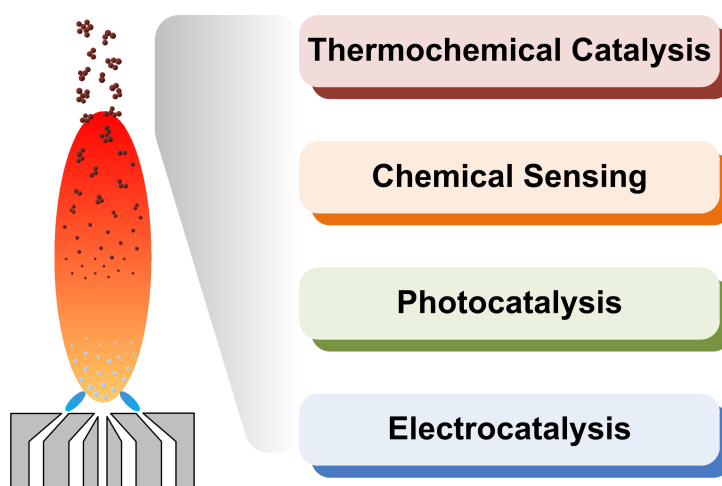
E-Mail: c4e@cam.ac.uk

World Wide Web: <http://como.cheng.cam.ac.uk/>



Abstract

Flame aerosol synthesis (FAS) has been in industrial use for mass production of nanoparticle commodities, and in recent years has been developed into a tool for economic synthesis of novel catalytic nanomaterials as its scalability and versatility became recognized. In particular, a wide spectrum of metal oxide and noble metal nanoparticles/composites have been obtained by flame spray pyrolysis (FSP) which have demonstrated applications in growing fields of catalysis such as CO₂ utilization, gas sensing and water splitting apart from traditional heterogeneous catalytic processes. However, current studies on the flame-synthesized nanocatalysts have largely remained phenomenological and design of the catalysts has been relatively unsophisticated for photo- and electrocatalytic applications, where ample opportunities for future research are found. It is believed that interfacing the two large fields of combustion and materials application will further motivate the advancement of combustion field, and benefit the materials community with an alternative and practical synthesis option. With this in mind, this article presents the most recent progress pertaining to such a linkage, which we hope to stimulate further and deeper interest in such cross-disciplinary efforts.



Highlights

- Flame aerosol synthesis (FAS) is suitable for commercial nanocatalyst production.
- Research on FAS has advanced fast into energy and environmental applications.
- FAS-made nanocatalysts have shown satisfactory real-world performance.
- Great opportunities for applications of FAS lie in photo- and electrocatalysis.

Contents

1	Introduction	3
2	Thermochemical catalysis	4
3	Chemical sensing	7
4	Photocatalysis	8
5	Electrocatalysis	11
6	Concluding remarks	12
7	Acknowledgments	12
	References	15

1 Introduction

Flame aerosol synthesis (FAS) is an industrially relevant technology for manufacture of nanoparticles. In essence, it involves a continuous flow process where precursors are introduced into a stable flame and particles form from gaseous pyrolysis products. A typical FAS process which was developed by Degussa for the manufacture of fumed silica is illustrated in **Figure 1**. With its earliest intentional use traceable to prehistoric times in the making of soot for cave paintings, FAS now accounts for the production of the majority of nanoparticle commodities including carbon black, fumed SiO_2 , pigmentary TiO_2 , and the benchmark photocatalyst TiO_2 P25 [61]. Meanwhile as nanoscale engineering and surface manipulation push the laboratory performance of heterogeneous catalysts to new levels, development of reliable methods to mass-produce such nanocatalysts becomes increasingly important in realizing their practical applications. Compared with the wet chemical methods that dominate current research on nanocatalysts, FAS requires fewer unit operations, shorter processing time and simpler waste treatment, and is easily scaled up, making itself an attractive option for large-scale manufacturing of catalysts [39]. For example, industrial FAS processes use cyclones and/or bag filters for product separation which have high throughput and minimal energy consumption [37, 62, 68]. The tail gas is treated with absorption towers to co-produce hydrochloric acid in chloride-fed processes (which are responsible for the commercial production of most oxide nanoparticles) [62, 68] or burnt in boilers for energy recovery in carbon black processes [37].

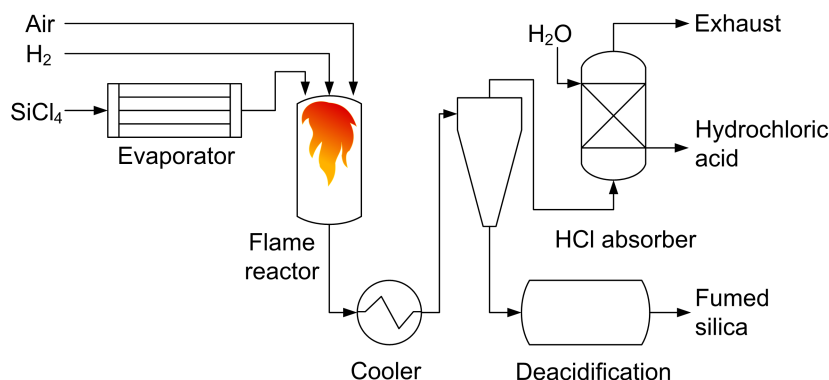


Figure 1: Simplified schematic representation of the AEROSIL[®] process for fumed silica production.

In the above context, flame aerosol reactors of various configurations have been developed, enabling the synthesis of carbon, noble metal and especially metal oxide nanoparticles/nanocomposites [39]. Basically, FAS can be classified into vapor-fed (VFAS) and liquid-fed (LFAS) types depending on the physical state of precursors upon entering the flame. While VFAS is adopted by the first commercial processes such as AEROSIL[®] due to low cost of suitable precursors (SiCl_4 and TiCl_4), the stringent requirement of VFAS on precursor volatility has since limited its use to the synthesis of mainly Al, Si, Ti, V, Fe, Zr and Sn oxides [39]. By far the most kinds of nanomaterials in terms of composition have been synthesized by FSP, the representative configuration of LFAS which allows for a wider selection of precursors. **Figure 2a** illustrates a basic FSP set-up used in laboratory research.

The fundamental understandings, reactor configurations, diagnostic techniques and product diversity of FAS have been extensively reviewed [30, 39, 44, 53, 57, 63]. The latest review focused on flame-synthesized catalytic nanomaterials is presented in Ref. [36], which covers works published by up to early 2015. However, the long history of FAS being studied as a branch of combustion science has hindered its exposure to the materials and catalysis communities, and the technology has been mainly reviewed in terms of the science of the synthesis process itself. As the development of flame-synthesized nanocatalysts continues to advance fast, we feel it appropriate now to highlight the most recent trends in this topic with an emphasis on emerging applications. Therefore, this mini-review mainly covers studies in the last two years which are broadly divided into four sections according to the type of catalytic application reported: thermochemical catalysis, chemical sensing, photocatalysis, and electrocatalysis.

2 Thermochemical catalysis

While catalysts for industrial processes such as steam reforming of methane and methanol synthesis have been well established, studies on new catalysts including those obtained by FAS are still ongoing. **Table 1** summarizes the recent works on FAS synthesized catalysts, the corresponding catalytic reactions and the optimized performances. One of the main strategies in nanocatalyst design for these reactions is the maximization of exposed active sites. In a rare example of using mixed-phase precursors in FSP, an Al_2O_3 -supported 1–3 nm Rh catalyst was obtained from combustion of a suspension containing dissolved Rh precursor and preformed AlOOH particles as shown in **Figure 2b** [71]. The catalyst showed higher methane reforming activity than those prepared from FSP of a homogeneous solution of soluble Rh and Al precursors. The discrepancy in metal dispersion calculated by chemisorption and TEM indicated that the use of the nonvolatile AlOOH prevented the incorporation of Rh nanoparticles in the bulk of Al_2O_3 support which occurred during concurrent gas-to-solid particle growth of Rh and Al_2O_3 from volatile precursors. In another effort to increase the active surface area, FSP synthesis of MCM-41 was attempted, probably for the first time, to disperse a Pd-Cu/ZnO methanol synthesis catalyst [56]. By combustion of an atomized 1:1 water/ethanol solution of cetyltrimethylammonium bromide, tetraethyl orthosilicate and sulfuric acid, MCM-41 was synthesized in the form of submicron spherical particles. Hexagonal pore ordering of the product was proven by XRD but its surface area and pore volume are about half of those obtained by sol-gel synthesis, which resulted in poorer catalyst dispersion during the following impregnation of Pd-Cu/ZnO. It should be noted, however, that large surface area obtained by flame synthesis is not always beneficial to activity, as evidenced in methane reforming over $\text{Ni/TiO}_2\text{-CeO}_2$ [31] and methanol synthesis over $\text{Cu/ZnO/Al}_2\text{O}_3$ [38] where crystallinity seems more important. For these nanocatalysts with increasingly complex structures, performance usually depends on the synergy between the surface chemistries of the support and active materials which makes separate control of the two phases desirable. To achieve this, sophisticated two-nozzle FSP has been adopted for catalyst synthesis. As illustrated in **Figure 2d**, the two nozzles are aimed at each other at an angle allowing early-stage particle formation in each spray to occur separately before the two streams of products merge. **Figure 2e** shows that the AuPd/TiO_2 alloy catalyst benefited from the simultane-

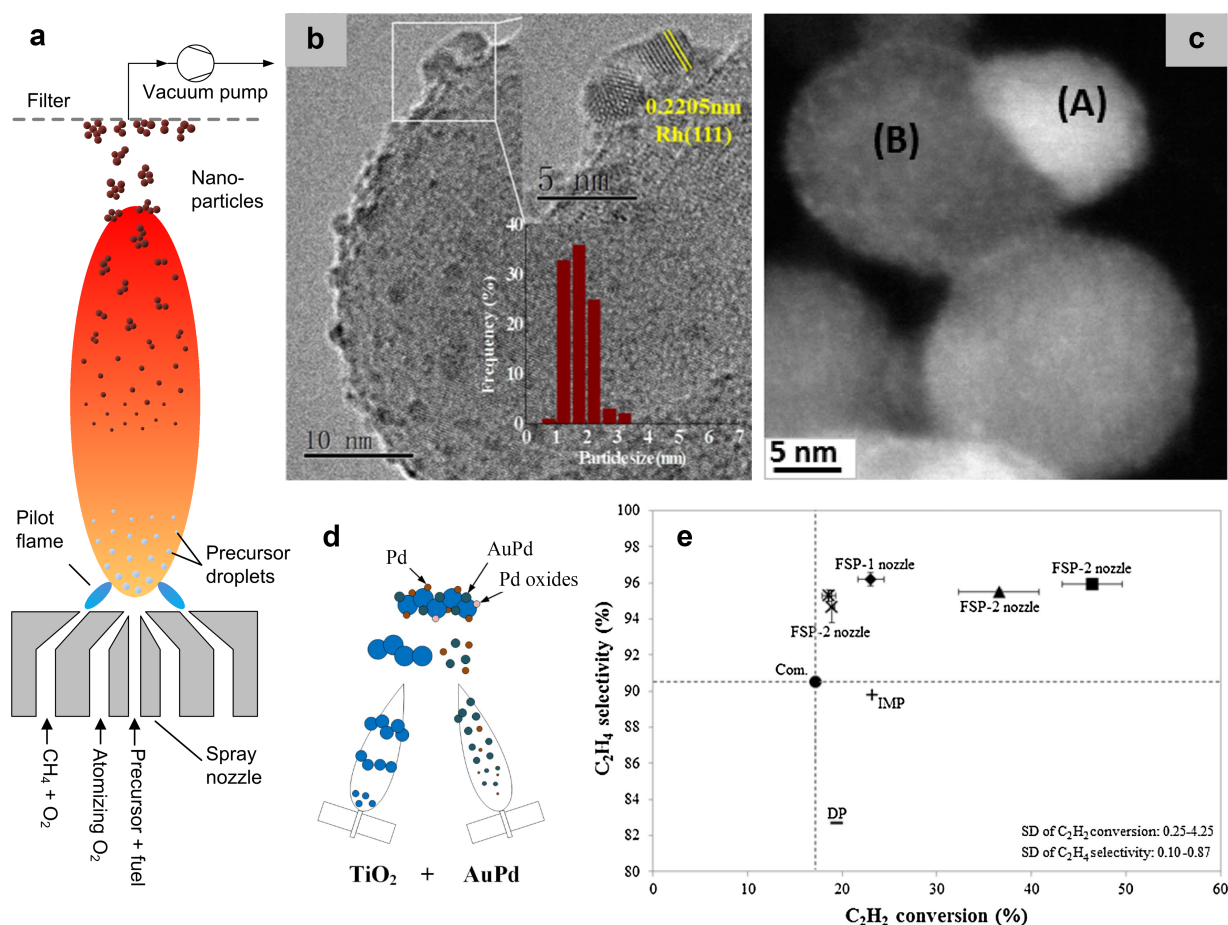


Figure 2: (a) Schematic representation of a typical laboratory configuration of FSP. (b) TEM image of a Al_2O_3 -supported Rh catalyst prepared by FSP. The insets show the lattice fringes and particle size distribution of the Rh particles. Reprinted from Ref. [71] with permission from Elsevier, Copyright (2016). (c) Dark-field STEM image of a CeO_x - TiO_2 -supported WO_3 catalyst synthesized by FSP. The support phase is Ti-doped CeO_x in region A and Ce-doped TiO_2 in region B. Reprinted from Ref. [45] with permission from American Chemical Society, Copyright (2015). (d) Schematic representation of the configurations used for the 2-nozzle FSP synthesis of Au-Pd- TiO_2 catalysts and (e) performance of the catalysts in acetylene hydrogenation at 40 °C. ◆: AuPd/ TiO_2 by one-nozzle FSP, ■: TiO_2 +AuPd, ▲: Au/ TiO_2 +Pd, ×: Pd/ TiO_2 +Au, ×: Pd/ TiO_2 +Au/ TiO_2 , ●: commercial PdAu/ TiO_2 , +: AuPd/ TiO_2 prepared by co-impregnation, -: AuPd/ TiO_2 prepared by co-deposition precipitation. Adapted and reprinted from Ref. [47] with permission from Elsevier, Copyright (2018).

ous control of metal-metal and metal-support interactions in selective hydrogenation of acetylene to ethylene [47]. It was found that separately feeding the Pd and Ti precursors in two nozzles prevented overly strong metal-support interaction which would otherwise cause oxidation of Pd, its coverage by Ti-O species, and hence fewer active sites. Meanwhile the co-feeding of Au and Pd precursors in one nozzle promoted formation of the

more active and selective AuPd alloy over pure Pd. Thus the TiO₂ + AuPd configuration afforded optimal catalytic performance. Remarkably, for the Pd/Al₂O₃-SiO₂ system a two-nozzle Pd + Al₂O₃-SiO₂ configuration allowed for more than quadrupling of turnover frequency in acetophenone hydrogenation without significant compromise in selectivity towards phenylethanol, the product of chemoselective hydrogenation [33]. By increasing the O₂/precursor ratio in the feed of the nozzle synthesizing the catalyst support, particle residence time and flame temperature were reduced, resulting in smaller particle size and higher density of surface hydroxyl groups with Brønsted acidity which activated the hydrogenation reaction. At the same time, the surface properties of the Pd particles formed in the other spray was relatively unaffected, which determined the selectivity.

Recently, attention to environmental issues related to fossil fuel consumption has led to an unprecedented scale of energy and environmental research, which is also reflected by the applications of flame-synthesized catalysts. As an apparent method to mitigate the greenhouse effect brought by CO₂, its chemical transformation by hydrogenation has become a major subject of interest. The practical value of CO₂ hydrogenation depends highly on its selectivity due to the diversity of possible products, demanding careful control of the adsorption of intermediates to manipulate reaction pathways. In this field, the application of flame-synthesized nanocatalysts has been focused on CO₂ methanation, the thermodynamically favored reaction at low temperatures. CH₄ selectivity of > 95% has been achieved at CO₂ conversions of > 80% on Ru/CeO₂ [13] and CoPt/Al₂O₃ [55] by optimizing metal-support interaction. The work on the Ru-based catalyst demonstrated the versatility of FSP in catalyst screening, as Ru/MnO_x, Ru/Al₂O₃, Ru/CeO₂ and Ru/ZnO with similar textural properties were synthesized by the same set-up. Reducibility of the support was found to significantly influence the strength of CO adsorption on Ru during reaction, the key factor in methanation activity. The mildly reduced CeO₂ afforded optimal CO adsorption that left enough surface Ru sites for H₂ dissociation while weakening the C=O bond for hydrogenation to CH₄. To prepare the CoPt/Al₂O₃ catalyst, a two-nozzle FSP separating the Co and Al precursors was used which avoided formation of inactive CoAl₂O₄ while ensuring high dispersion of reducible Co₃O₄ and hence good activity (metallic Co was the active species during reaction). The reducibility of Co₃O₄ was further improved by doping of as low as 0.03 wt% of Pt during FSP, bringing the performance comparable to that achieved by precious metal catalysts. Besides hydrogen, hydrocarbons can also act as the reducing agent in CO₂ conversion. However, compared with the weak H-H bond in H₂, the activation of C-H bonds in hydrocarbons requires significantly higher temperature and is accompanied by coking, which makes the stability of the catalyst an important consideration. For example, the thermal stability of a Ni-based catalyst for dry reforming of CH₄ was enhanced by a large degree of Si doping in the Si_xCe_{0.7}Zr_{0.3}O_y support material, improving catalyst deactivation at 700 °C [42]. In CO₂-assisted oxidative dehydrogenation of ethane on a Co/SiO₂ catalyst, resistance to sintering was achieved by formation of CoSiO₃ as the pre-catalyst during FSP [35]. As evidenced by the high temperature of ~700 °C where reduction of the pre-catalyst started during temperature-programmed reduction in 5% H₂/Ar, the formation of CoSiO₃ provided strong metal-support interaction that stabilized the active Co particles during reaction. At 700 °C, the catalyst exhibited stable performance of 80% selectivity towards ethylene at 30% conversion during a 5 h test. In addition, petrochemical production from alternative fossil-based feedstock, e.g. Fischer-Tropsch process [11] and

oxidative CH₄ coupling [14] have been demonstrated using flame-synthesized Co/SiO₂ and La₂O₂CO₃/La₂O₃ catalysts, respectively. It is worth noting that liquid dispersion during FSP plays a crucial role in controlling phase composition of resulting nanoparticles, as shown in the synthesis of La₂O₂CO₃/La₂O₃ where an optimal combination of phases for oxidative CH₄ coupling activity was obtained at low liquid dispersion by feeding La precursor as a viscous microemulsion [14].

Exhaust treatment has formed another field of application of flame-synthesized catalysts. For example, to selectively reduce NO_x to N₂ with NH₃, a highly dispersed WO₃/CeO_x-TiO₂ catalyst was fabricated by FSP [45]. Due to the high vapor pressure of WO₃ and its low solubility in the support oxides, WO₃ nucleated late in the cooler zones of the flame during FSP and deposited only on the surface of CeO_x-TiO₂ as sub-nano clusters despite a high WO₃ loading of 10 wt% (**Figure 2c**). Benefitting from surface Ce³⁺ generated by the Ti⁴⁺ doping, the performance of the catalyst is comparable to the more widely used V₂O₅-WO₃/TiO₂ catalyst without the drawback of releasing toxic V species. The same application was also demonstrated using a V-doped TiO₂ catalyst obtained by VFAS, where titanium tetraisopropoxide (TTIP) and vanadium oxytriisopropoxide vapors were introduced to a premixed CH₄/O₂ flame [6]. We highlight here a study on FSP synthesis of Cu_{1.5}Mn_{1.5}O₄ nanocatalyst for low-temperature CO oxidation [4]. The unique features of FAS, i.e. fast quenching and facile co-formation of carbonaceous species, were utilized to stabilize the metastable Cu_{1.5}Mn_{1.5}O₄ phase and decrease its surface hydrophilicity, respectively. The resulting catalyst has similar activity as that of a commercial benchmark and a much higher durability against moisture. In a more radical way of reducing NO_x and CO emission by decreasing the combustion temperature, a series of works on catalytic combustion of methane have also been done using supported Pd catalysts [64, 65, 74], where strong metal-support interaction with reducible CeO₂/TiO₂ supports provided high metal dispersion and resistance to Pd sintering. Modelling efforts have shown that the TiO₂ precursor (TTIP) decomposes much faster than the Pd precursor in flame, and TiO₂ seed particles may have already formed where Pd only exists as monomeric vapor [43, 74]. The growing TiO₂ particles can scavenge Pd clusters at a faster rate than the decomposition of Pd precursor, hence limiting its particle growth.

3 Chemical sensing

Typically in FAS, the flame operates in open atmosphere and particle movement is guided by feed gas flows which can be easily directed towards various substrates for deposition of porous nanostructured films. Therefore, FAS is particularly suitable for fabrication of flat devices that require large surface areas, chemical sensors being a good example. During the past three years, metal-oxide semiconductor (MOS) gas sensors have been the focus of studies on flame-synthesized materials for chemical sensing, as summarized in **Table 2**. This class of sensors rely on adsorption and catalytic reaction of gas species on the surface of semiconductor particles to change the height of electronic barrier at particle-particle contacts and hence current flow across the device. It can be seen that for high sensitivity, participation of a large number of particle interfaces in current flow and a large active surface area are needed. In this regard, size reduction of the nanoparticles during FAS has

been proven a successful strategy [5, 18, 26, 48, 54, 58]. For example, a FSP-synthesized SnO₂:Sb sensor consisting of 9–17 nm particles has shown a response to ethanol that is at least an order of magnitude higher compared with similar sensors prepared by wet chemical methods [5]. A problem with using small nanoparticles is loss of performance by sintering, because the sensing film usually has to operate at elevated temperatures for optimal response [25]. Stabilization of the particle-particle interfaces by doping and passivation of inert phases seems to be a viable solution, as in the Si-doped α -MoO₃ NH₃ sensor [18]. Moreover, dramatic improvement in sensor response has been reported by mixing the semiconductor particles with graphene materials either by post-processing [48, 59] or co-spraying [41]. The underlying mechanism of performance enhancement may be related to graphene-semiconductor electron transfer and/or selective adsorption properties of graphene.

For reliable gas detection, selectivity of the sensor is the most important criterion. In contrast to sensitivity, selectivity of a certain sensor material is usually independent on its textural properties and has to be optimized by tuning its intrinsic chemical properties. So far the choice of materials in MOS sensors has been limited to several simple oxides, which necessitates various dopants for tailored sensor performance (**Table 2**). A notable example is the doping of Si in WO₃, whereby a metastable ϵ -WO₃ phase was captured by FSP and exhibited high selectivity towards acetone sensing [50], allowing accurate determination of acetone concentration in human breath during clinical study [19]. Instead of seeking materials with exceptional intrinsic selectivity, the “electronic nose” approach has also been adopted utilizing an array of four differently doped SnO₂ sensors, the structure of which is shown in **Figure 3a–c** [17]. Using multivariable regression analysis of the different response of the four sensors, quantification of formaldehyde down to 30 ppb with an error of ≤ 9 ppb was possible in simulated breath mixture containing acetone, NH₃, ethanol and moisture. Importantly, large-scale sensor production and integration were demonstrated in the same work. Unfortunately, surface adsorption and catalytic reactions which dictate sensor performance have received little detailed investigation during the research on flame-synthesized gas sensors. More in-depth studies are necessary to reveal the influence of the intrinsic and surface properties of the sensing materials on the adsorption and reaction processes, so as to achieve better materials design.

Apart from gas sensing, electrochemical detection of biochemicals such as glucose [27], methyl parathion [28] and caffeic acid [29] in aqueous phase has also been studied using flame-synthesized materials. These works exploited the flexibility in fuel selection to prepare nanosized carbon doped with N or S in open flames of heterocyclic compounds. Through cyclic voltammetry experiments in standard 3-electrode cells, lower detection limits in the nM scale have been achieved by these electrochemical sensors, as seen in their performance in realistic samples [27–29].

4 Photocatalysis

The rationale of developing photocatalytic processes is that direct utilization of sunlight as the driving force for chemical reactions minimizes environmental impact and potentially renders the process independent of fossil energies. Therefore, the main application

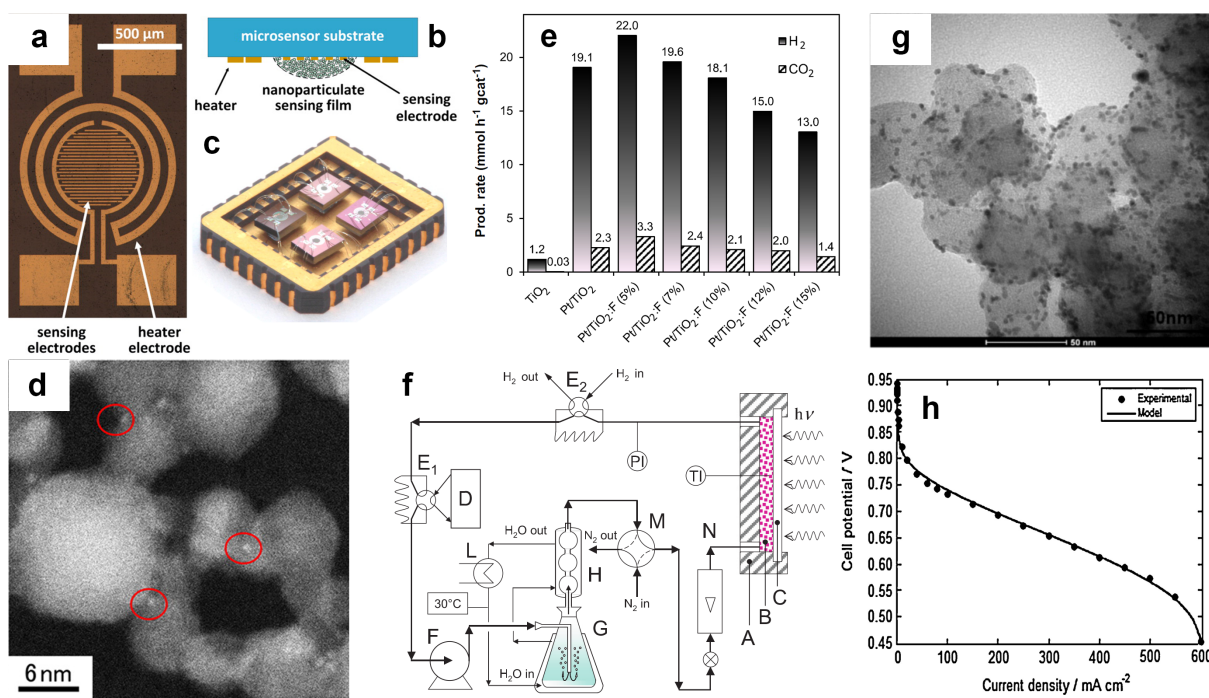


Figure 3: (a) Photograph of the substrate patterned by Pt electrodes used to prepare (b) individual Pt-, Si-, Pd-, or Ti-doped SnO₂ sensors by FSP and (c) integrated electronic nose device consisting of the four types of sensors. Reprinted from Ref. [17] with permission from American Chemical Society, Copyright (2016). (d) Dark-field STEM image of TiO₂-supported sub-nanometer Pd clusters synthesized by FSP. Some Pd clusters are highlighted by red circles. Reprinted from Ref. [16] with permission from American Chemical Society, Copyright (2016). (e) H₂ and CO₂ production rates during photocatalytic methanol reforming on FSP-made Pt/TiO₂:F catalysts. Reprinted from Ref. [8] with permission from Elsevier, Copyright (2014). The photocatalytic performance was evaluated in the set-up illustrated in (f) where A: Plexiglas photoreactor; B: photocatalyst bed; C: Pyrex-glass window; D: detector; E₁, E₂: six-way sampling valves; F: bellows pump; G: methanol/water bubbler; H: condenser; L: thermostat; M: four-way ball valve; N: gas flowmeter; TI: temperature indicator; PI: pressure indicator. Reprinted from Ref. [7] with permission from Elsevier, Copyright (2009). (g) TEM image of a Pt/CB/PTFE catalyst prepared by post-flame co-spraying of CB/PTFE support slurry during FSP synthesis of Pt. (h) Optimal performance of the H₂/O₂ fuel cell constructed using the Pt/CB/PTFE catalyst directly deposited on gas diffusion layers. Reprinted from Ref. [34] with permission from Elsevier, Copyright (2015).

of photocatalysts has been in energy and environmental technologies. Generally, small particle size provided by FAS is beneficial as it reduces the path of charge carrier diffusion and hence the chance of recombination, but the low crystallinity and abundant defects associated with fast quenching might, on the other hand, promote recombination and decrease the catalyst's performance [66]. So far, environmental remediation has been

the most intensively studied application of flame-synthesized photocatalysts. In this field, TiO₂ forms the base material of a majority of works because it is readily mass-produced as nanoparticles by FAS at low cost. However the wide band gap of TiO₂ does not allow absorption of visible light, making it an intrinsically inefficient photocatalyst under sunlight, and thus research on pure TiO₂ has declined recently. Nevertheless, the few works focused on flame-synthesized pure TiO₂ demonstrated the importance of optimal phase composition to fast degradation of organic contaminants [2, 3], which may be a manifestation of the slightly narrower band gap and hence better light absorption of rutile TiO₂ compared with anatase TiO₂. Most frequently, TiO₂ is doped with noble metals [15, 16, 46], 3d transition metal cations [21, 22], or nonmetal anions having similar ionic radius as O²⁻ [12, 67] for enhanced performance. Noble metals do not usually enter the crystal structure of TiO₂ but form deposits on its surface due to incompatibility in lattice constants. The noble metal particles improve carrier separation by trapping photo-generated electrons, provide new catalytic centers, and may allow visible light absorption through localized surface plasmon resonance [46]. Notably, sub-nanometer Pd clusters and single-atom Pd catalysts supported on TiO₂ have been developed by FSP (**Figure 3d**) that minimize noble metal loading and compare favorably with wet-chemically prepared analogues in photocatalytic NO_x removal [15, 16]. As a cheaper alternative to noble metals, 3d transition metal dopants can also extend the absorption spectrum of TiO₂ in the visible region and catalyze surface reactions [20]. For water treatment, a special concern is leaching of the dopant which is often a pollutant by itself and co-doping of Si during FSP was found effective in preventing such leaching [21, 22]. In a different approach to performance enhancement of TiO₂ photocatalyst, F dopant was introduced during FSP to alter the distribution of surface hydroxyl groups and hence catalytic reaction pathways with practically no effect on the optical properties of TiO₂ [12, 67]. Apart from TiO₂, flame-synthesized WO₃ has received some attention due to its intrinsic sensitivity to visible light [1, 66]. One of the studies used polystyrene nanospheres as sacrificial template in the precursor mixture to generate well-defined macropores in WO₃ particles during FSP [1], an interesting strategy of morphological control whose use has largely been limited to wet-chemical synthesis. However, the higher cost of WO₃ compared with TiO₂ is a significant drawback in air/water treatment, a low value-added process.

In contrast to air/water treatment, other potential applications of flame-synthesized photocatalysts such as water splitting and CO₂ reduction have attracted far less research recently [9, 10, 60, 69]. As the surface chemistry of commonly used photocatalysts, e.g. TiO₂, is not optimal for the mentioned reactions, a co-catalyst is usually required to achieve decent overall quantum yield. For example, deposition of noble metals, particularly Pt which is one of the most efficient hydrogen evolution catalysts, on TiO₂ nanoparticles during FSP has been proven a highly effective method of enhancing their activity in photocatalytic hydrogen production [9]. In a vapor-phase photocatalytic methanol steam reforming reactor shown in **Figure 3f**, the latest development of the Pt/TiO₂ system involving co-doping of F has demonstrated a hydrogen production rate of up to 22 mmol/g_{cat}·h under a 300 W Xe arc lamp (**Figure 3e**) [8]. Alternatively, the co-catalyst can be another semiconductor that facilitates carrier separation by forming heterojunctions, as in the case of photocatalytic CO₂ reduction on a ZnO/CeO₂ composite catalyst [69]. However, the quantum yield was still low (< 1%) over the full UV-vis spectrum of a 300 W Xe lamp. Finally, it should be mentioned that the combination of wet-chemical and flame synthesis in the so-called

“sol-flame” method has led to Ti-doped Fe_2O_3 water oxidation photoanodes with considerable morphological control that is difficult by FAS alone [10]. Although the flame was only used as a heat source in this work, it can be envisaged that introduction of metal precursors to the flame treatment will enable the fabrication of structurally more complex nanocatalysts/devices.

5 Electrocatalysis

Among the applications covered in this review, electrocatalysis of flame-synthesized materials has been the least frequently studied which contrasts with the current intensive research on oxygen/hydrogen evolution reactions (OER/HER), oxygen reduction reaction (ORR), and electrochemical CO_2 reduction in general. It is surprising given that some of the best wet-chemically synthesized catalysts for the above reactions such as Pt, Ru, Fe/Co/Ni oxides and Cu oxides have been successfully prepared by FAS [39]. Recent research in this field have been mainly focused on precious metals for water splitting [32, 51] and fuel cells [34, 52], with works on CO_2 reduction yet to be found. Nevertheless, important application-oriented studies have been carried out where electrodes ready to use in practical fuel cell / water electrolyzer set-ups were fabricated by simultaneous deposition of FSP-synthesized Pt nanoparticles, conducting carbon black (CB) and perfluorinated polymeric binders [34, 51]. The CB support and binder were sprayed into the relatively cool post-flame region of the Pt-forming flame, where the temperature is high enough to encourage interaction between Pt and CB while not causing decomposition of the polymer binder. The Pt particles in such catalyst films are evenly distributed on the CB support as shown in **Figure 3g** and exhibit high electrochemical activity. For example, a high-temperature proton exchange membrane H_2/O_2 fuel cell constructed from as-made $5 \times 5 \text{ cm}^2$ Pt/CB/polytetrafluoroethylene (PTFE) gas diffusion electrodes and commercial Advent TPS[®] membrane exhibited cell performance of practical significance at the low total Pt loading of 0.1 mg/cm^2 and a temperature of $190 \text{ }^\circ\text{C}$ (**Figure 3h**) [34]. Reasonable accuracy was also obtained by preliminary performance modelling. The same group developed a Pt/CB/Nafion HER electrode with a loading of 0.4 mg/cm^2 which showed similar performance as an industrial-quality electrode at current densities up to 2 A/cm^2 in proton exchange membrane electrolysis, with less than 40 mV increase in cell voltage after 1075 h of durability test at 1.86 A/cm^2 [51]. A combined computational/experimental study on flame synthesis and OER activity of Ru-based perovskites [32] is also interesting in the sense that it illustrated possibilities of theory-guided design of flame-synthesized nanocatalysts. In comparison, application of flame-synthesized earth-abundant materials in water electrolysis has remained in the proof-of-concept stage. A rare example demonstrated an OER overpotential of 0.41 V at 10 mA/cm^2 and Tafel slope of 99 mV/dec in 1 M NaOH electrolyte solution on a Mn_2O_3 nanoparticle electrode prepared by FSP deposition and thermal treatment [40].

6 Concluding remarks

In the past two years, a considerable amount of research has been carried out on the application of flame-synthesized nanocatalysts in emerging fields of catalysis such as CO₂ utilization, gas sensing and water splitting. With its high throughput and capability of fast device manufacturing, FAS continues to be a potentially economic method for large-scale production of nanocatalysts. Such possibility has been demonstrated by the high performance of some flame-synthesized gas sensors and water electrolysis electrodes in realistic environments. However, while an increasing level of sophistication has been seen in the design, synthesis and characterization of such materials for conventional heterogeneous catalysis, the exploration of novel flame-synthesized catalysts for photo-/electrocatalytic applications and corresponding detailed mechanistic studies have been very limited. Particularly, facile formation of carbonaceous materials in flames could be a valuable tool for the modification of poorly conductive electrocatalysts [72, 73] or preparation of metal-free electrocatalysts [70], but has received little attention. We believe that great opportunities of future research exist in these directions.

7 Acknowledgments

The authors acknowledge the financial support of the Singapore National Research Foundation (NRF) through the Campus for Research Excellence and Technological Enterprise (CREATE) program.

Table 1: Recent studies on thermochemical catalysis using flame-synthesized nanocatalysts

Catalyst	Reaction	Reaction condition ^a	Optimal performance	Ref.
Rh/Al ₂ O ₃	CH ₄ steam reforming	600 °C, 100 kPa, H ₂ O/CH ₄ = 4, GHSV = 60 L CH ₄ /g _{cat} ·h	69% CH ₄ conversion, TOF = 22 s ⁻¹	[71]
PdCu/ZnO/MCM-41	Methanol synthesis from CO ₂	250 °C, 25 bar, H ₂ /CO ₂ = 3, GHSV = 1800 h ⁻¹	24% CO ₂ conversion, 2% methanol selectivity	[56]
Ni/TiO ₂ -CeO ₂	CH ₄ steam reforming	500 °C, 1 atm, H ₂ O/CH ₄ = 1, GHSV = 6 L CH ₄ /g _{cat} ·h	~57 mmol CH ₄ /g _{cat} ·h, selectivity: ~90% H ₂ , ~60% CO ₂ , ~20% CO	[31]
Cu/ZnO/Al ₂ O ₃ + HZSM-5	Direct dimethyl ether (DME) synthesis	260 °C, 40 bar, H ₂ :CO:CO ₂ = 16:8:1, 10% N ₂ , GHSV = 0.9 L/g _{cat} ·h	~91% CO conversion, ~62% DME selectivity	[38]
AuPd/TiO ₂	C ₂ H ₂ hydrogenation	40 °C, 1 atm, 1.5% C ₂ H ₂ , 2% H ₂ in C ₂ H ₄ , GHSV = 120 L/g _{cat} ·h	~46% C ₂ H ₂ conversion, ~96% C ₂ H ₄ selectivity	[47]
Pd/Al ₂ O ₃ -SiO ₂	Acetophenone hydrogenation	15 °C, 3 bar, 3 h, 60 mg acetophenone in 6 mL hexane, Pd/acetophenone = 1/101 (mol/mol)	100% acetophenone conversion, 88% phenylethanol selectivity, TOF = 0.05 s ⁻¹	[33]
Ru/CeO ₂	CO ₂ methanation	300 °C, 1 atm, 22% H ₂ , 4.6% CO ₂ in Ar, GHSV = 7640 h ⁻¹	83% CO ₂ conversion, 99% CH ₄ selectivity	[13]
CoPt/Al ₂ O ₃	CO ₂ methanation	400 °C, 100 kPa, H ₂ /CO ₂ = 4	70% CO ₂ conversion, 98% CH ₄ selectivity	[55]
Ni/Si _x Ce _{0.7} Zr _{0.3} O _y	CH ₄ dry reforming	700 °C, 1 atm, CH ₄ :CO ₂ :N ₂ = 1:1:1, GHSV = 144 L/g _{cat} ·h	~50% CH ₄ conversion, H ₂ /CO ≈ 1	[42]
Co/SiO ₂	CO ₂ -assisted oxidative C ₂ H ₆ dehydrogenation	700 °C, 1 atm, CO ₂ /C ₂ H ₆ = 2.5, GHSV = 6 L/g _{cat} ·h	30% C ₂ H ₆ conversion, 80% C ₂ H ₄ selectivity	[35]
Co/SiO ₂	Fischer-Tropsch synthesis	260 °C, 20 bar, H ₂ /CO = 2, GHSV = 3 L/g _{cat} ·h	~98% CO conversion, selectivity: 11% CH ₄ , 10% <C ₇ , 73% >C ₇	[11]
La ₂ O ₂ CO ₃ /La ₂ O ₃	Oxidative CH ₄ coupling	650 °C, CH ₄ /O ₂ = 2, 10% N ₂	44% CH ₄ conversion, ~13% C ₂ yield	[14]
WO ₃ /CeO _x -TiO ₂	Selective NO _x reduction by NH ₃	250 °C, 1 atm, 10% O ₂ , 5% H ₂ O, 1000 ppm NO, 1200 ppm NH ₃ in N ₂ , GHSV = 120 L/g _{cat} ·h	~100% NO _x conversion, 100% N ₂ selectivity	[45]
Ti _{0.9} V _{0.1} O _{2-δ}	Selective NO _x reduction by NH ₃	250 °C, 1 atm, 5% O ₂ , 5% H ₂ O, 600 ppm NO, 600 ppm NH ₃ in N ₂ , GHSV = 90,000 L ⁻¹	100% NO _x conversion, ~100% N ₂ selectivity	[6]
Cu _{1.5} Mn _{1.5} O ₄	CO oxidation	120 °C, 1 atm, 0.67% CO, 33.33% O ₂ in N ₂ , GHSV = 40 L/g _{cat} ·h	100% CO conversion	[4]
Pd/TiO ₂	Catalytic CH ₄ combustion	572 °C, 1 atm, 8% O ₂ , 2% CH ₄ in N ₂	85.7% CH ₄ conversion	[74]
Pd/CeO ₂	Catalytic CH ₄ combustion	~570 °C, 1 atm, 8% O ₂ , 2% CH ₄ in N ₂ , GHSV = 520 L/g _{cat} ·h	~65% CH ₄ conversion	[64]
Pd/CeO ₂ -TiO ₂	Catalytic CH ₄ combustion	470 °C, 1 atm, 8% O ₂ , 2% CH ₄ in N ₂ , GHSV = 260 L/g _{cat} ·h	100% CH ₄ conversion	[65]

^a GHSV: gas hourly space velocity

Table 2: *Recent studies on gas sensing using flame-synthesized semiconductor nanocatalysts*

Host material	Dopant	Target gas	Calculated lower detection limit (ppb)	Ref.
SnO ₂ /graphene	None	NO ₂	10	[59]
SnO ₂	Sb	Ethanol	<1000	[5]
SnO ₂	Si, Ti, Pd, Pt	Formaldehyde	3	[17]
SnO ₂ /graphene	Co	Ethanol	700	[48]
SnO ₂	Sb-Pt, Pd	Ethanol/CO	N.A.	[49]
SnO ₂	Rh	H ₂	2000	[24]
SnO ₂	Mo	H ₂ S	80	[26]
SnO ₂	V	H ₂ S	80	[58]
γ-WO ₃	None	NO ₂	<170	[25]
ε-WO ₃	Si	Acetone	20	[50]
WO ₃ /graphene	None	O ₃	500	[41]
α-MoO ₃	Si	NH ₃	400	[18]
ZnO/In ₂ O ₃	None	NO ₂	20	[54]
In ₂ O ₃	Nb, Ru, Pt	NO ₂	<125	[23]

References

- [1] O. Arutanti, A. F. Arif, R. Balgis, T. Ogi, K. Okuyama, and F. Iskandar. Tailored synthesis of macroporous Pt/WO₃ photocatalyst with nanoaggregates via flame assisted spray pyrolysis. *AIChE J.*, 62(11):3864–3873, 2016. ISSN 00011541. doi:10.1002/aic.15349.
- [2] L. G. Bettini, M. V. Dozzi, F. D. Foglia, G. L. Chiarello, E. Selli, C. Lenardi, P. Piseri, and P. Milani. Mixed-phase nanocrystalline TiO₂ photocatalysts produced by flame spray pyrolysis. *Appl. Catal., B*, 178:226–232, 2015. ISSN 09263373. doi:10.1016/j.apcatb.2014.09.013.
- [3] L. G. Bettini, M. V. Diamanti, M. Sansotera, M. P. Pedferri, W. Navarrini, and P. Milani. Immobilized TiO₂ nanoparticles produced by flame spray for photocatalytic water remediation. *J. Nanopart. Res.*, 18(8):238, 2016. ISSN 1388-0764 1572-896X. doi:10.1007/s11051-016-3551-6.
- [4] T. Biemelt, K. Wegner, J. Teichert, M. R. Lohe, J. Martin, J. Grothe, and S. Kaskel. Hopcalite nanoparticle catalysts with high water vapour stability for catalytic oxidation of carbon monoxide. *Appl. Catal., B*, 184:208–215, 2016. ISSN 09263373. doi:10.1016/j.apcatb.2015.11.008.
- [5] C. O. Blattmann, A. T. Guntner, and S. E. Pratsinis. In situ monitoring of the deposition of flame-made chemoresistive gas-sensing films. *ACS Appl. Mater. Interfaces*, 9(28):23926–23933, 2017. ISSN 1944-8252 (Electronic) 1944-8244 (Linking). doi:10.1021/acsami.7b04530.
- [6] T. Chen, H. Lin, B. Guan, X. Gong, K. Li, and Z. Huang. Promoting the low temperature activity of Ti-V-O catalysts by premixed flame synthesis. *Chem. Eng. J.*, 296:45–55, 2016. ISSN 13858947. doi:10.1016/j.cej.2015.08.115.
- [7] G. L. Chiarello, L. Forni, and E. Selli. Photocatalytic hydrogen production by liquid- and gas-phase reforming of CH₃OH over flame-made TiO₂ and Au/TiO₂. *Catal. Today*, 144(1-2):69–74, 2009. ISSN 09205861. doi:10.1016/j.cattod.2009.01.023.
- [8] G. L. Chiarello, M. V. Dozzi, M. Scavini, J.-D. Grunwaldt, and E. Selli. One step flame-made fluorinated Pt/TiO₂ photocatalysts for hydrogen production. *Appl. Catal., B*, 160-161:144–151, 2014. ISSN 09263373. doi:10.1016/j.apcatb.2014.05.006.
- [9] G. L. Chiarello, M. V. Dozzi, and E. Selli. TiO₂-based materials for photocatalytic hydrogen production. *J. Energy Chem.*, 26(2):250–258, 2017. ISSN 20954956. doi:10.1016/j.jechem.2017.02.005.
- [10] I. S. Cho, H. S. Han, M. Logar, J. Park, and X. Zheng. Enhancing low-bias performance of hematite photoanodes for solar water splitting by simultaneous reduction of bulk, interface, and surface recombination pathways. *Adv. Energy Mater.*, 6(4): 1501840, 2016. ISSN 16146832. doi:10.1002/aenm.201501840.

- [11] A. Comazzi, C. Pirola, A. Di Michele, M. Compagnoni, F. Galli, I. Rossetti, F. Marenti, and C. L. Bianchi. Flame spray pyrolysis as fine preparation technique for stable Co and Co/Ru based catalysts for FT process. *Appl. Catal., A*, 520:92–98, 2016. ISSN 0926860X. doi:10.1016/j.apcata.2016.04.010.
- [12] M. V. Dozzi, A. Zuliani, I. Grigioni, G. L. Chiarello, L. Meda, and E. Selli. Photocatalytic activity of one step flame-made fluorine doped TiO₂. *Appl. Catal., A*, 521: 220–226, 2016. ISSN 0926860X. doi:10.1016/j.apcata.2015.10.048.
- [13] J. A. H. Dreyer, P. Li, L. Zhang, G. K. Beh, R. Zhang, P. H. L. Sit, and W. Y. Teoh. Influence of the oxide support reducibility on the CO₂ methanation over ru-based catalysts. *Appl. Catal., B*, 219:715–726, 2017. ISSN 09263373. doi:10.1016/j.apcatb.2017.08.011.
- [14] C. Estruch Bosch, M. P. Copley, T. Eralp, E. Bilbé, J. W. Thybaut, G. B. Marin, and P. Collier. Tailoring the physical and catalytic properties of lanthanum oxycarbonate nanoparticles. *Appl. Catal., A*, 536:104–112, 2017. ISSN 0926860X. doi:10.1016/j.apcata.2017.01.019.
- [15] K. Fujiwara and S. E. Pratsinis. Atomically dispersed Pd on nanostructured TiO₂ for NO removal by solar light. *AIChE J.*, 63(1):139–146, 2017. ISSN 00011541. doi:10.1002/aic.15495.
- [16] K. Fujiwara, U. Müller, and S. E. Pratsinis. Pd subnano-clusters on TiO₂ for solar-light removal of NO. *ACS Catal.*, 6(3):1887–1893, 2016. ISSN 2155-5435 2155-5435. doi:10.1021/acscatal.5b02685.
- [17] A. T. Güntner, V. Koren, K. Chikkadi, M. Righettoni, and S. E. Pratsinis. E-nose sensing of low-ppb formaldehyde in gas mixtures at high relative humidity for breath screening of lung cancer? *ACS Sens.*, 1(5):528–535, 2016. ISSN 2379-3694 2379-3694. doi:10.1021/acssensors.6b00008.
- [18] A. T. Güntner, M. Righettoni, and S. E. Pratsinis. Selective sensing of NH₃ by Si-doped α -MoO₃ for breath analysis. *Sens. Actuators, B*, 223:266–273, 2016. ISSN 09254005. doi:10.1016/j.snb.2015.09.094.
- [19] A. T. Güntner, N. A. Sievi, S. J. Theodore, T. Gulich, M. Kohler, and S. E. Pratsinis. Noninvasive body fat burn monitoring from exhaled acetone with Si-doped WO₃-sensing nanoparticles. *Anal. Chem.*, 89(19):10578–10584, 2017. ISSN 1520-6882 (Electronic) 0003-2700 (Linking). doi:10.1021/acs.analchem.7b02843.
- [20] S. N. R. Inturi, T. Boningari, M. Suidan, and P. G. Smirniotis. Visible-light-induced photodegradation of gas phase acetonitrile using aerosol-made transition metal (V, Cr, Fe, Co, Mn, Mo, Ni, Cu, Y, Ce, and Zr) doped TiO₂. *Appl. Catal., B*, 144: 333–342, 2014. ISSN 09263373. doi:10.1016/j.apcatb.2013.07.032.
- [21] S. N. R. Inturi, T. Boningari, M. Suidan, and P. G. Smirniotis. Stabilization of Cr in Ti/Si/Cr ternary composites by aerosol flame spray-assisted synthesis for visible-light-driven photocatalysis. *Ind. Eng. Chem. Res.*, 55(46):11839–11849, 2016. ISSN 0888-5885 1520-5045. doi:10.1021/acs.iecr.6b02947.

- [22] S. N. R. Inturi, M. Suidan, and P. G. Smirniotis. Influence of synthesis method on leaching of the Cr-TiO₂ catalyst for visible light liquid phase photocatalysis and their stability. *Appl. Catal., B*, 180:351–361, 2016. ISSN 09263373. doi:10.1016/j.apcatb.2015.05.046.
- [23] K. Inyawilert, D. Channei, N. Tamaekong, C. Liewhiran, A. Wisitsoraat, A. Tuantranont, and S. Phanichphant. Pt-doped In₂O₃ nanoparticles prepared by flame spray pyrolysis for NO₂ sensing. *J. Nanopart. Res.*, 18(2):40, 2016. ISSN 1388-0764 1572-896X. doi:10.1007/s11051-016-3341-1.
- [24] K. Inyawilert, A. Wisitsoraat, A. Tuantranont, S. Phanichphant, and C. Liewhiran. Ultra-sensitive and highly selective H₂ sensors based on FSP-made Rh-substituted SnO₂ sensing films. *Sens. Actuators, B*, 240:1141–1152, 2017. ISSN 09254005. doi:10.1016/j.snb.2016.09.094.
- [25] R. Jain, Y. Lei, and R. Maric. Ultra-low NO₂ detection by gamma WO₃ synthesized by reactive spray deposition technology. *Sens. Actuators, B*, 236:163–172, 2016. ISSN 09254005. doi:10.1016/j.snb.2016.05.134.
- [26] S. Kabcum, N. Tammanoon, A. Wisitsoraat, A. Tuantranont, S. Phanichphant, and C. Liewhiran. Role of molybdenum substitutional dopants on H₂S-sensing enhancement of flame-spray-made SnO₂ nanoparticulate thick films. *Sens. Actuators, B*, 235:678–690, 2016. ISSN 09254005. doi:10.1016/j.snb.2016.05.129.
- [27] N. Karikalan, M. Velmurugan, S. M. Chen, and C. Karuppiah. Modern approach to the synthesis of Ni(OH)₂ decorated sulfur doped carbon nanoparticles for the nonenzymatic glucose sensor. *ACS Appl. Mater. Interfaces*, 8(34):22545–22553, 2016. ISSN 1944-8252 (Electronic) 1944-8244 (Linking). doi:10.1021/acsami.6b07260.
- [28] N. Karikalan, M. Velmurugan, S.-M. Chen, C. Karuppiah, K. M. Al-Anazi, M. A. Ali, and B.-S. Lou. Flame synthesis of nitrogen doped carbon for the oxygen reduction reaction and non-enzymatic methyl parathion sensor. *RSC Adv.*, 6(75):71507–71516, 2016. ISSN 2046-2069. doi:10.1039/c6ra10130e.
- [29] N. Karikalan, R. Karthik, S. M. Chen, and H. A. Chen. A voltammetric determination of caffeic acid in red wines based on the nitrogen doped carbon modified glassy carbon electrode. *Sci. Rep.*, 7:45924, 2017. ISSN 2045-2322 (Electronic) 2045-2322 (Linking). doi:10.1038/srep45924.
- [30] G. A. Kelesidis, E. Goudeli, and S. E. Pratsinis. Flame synthesis of functional nanostructured materials and devices: Surface growth and aggregation. *Proc. Combust. Inst.*, 36(1):29–50, 2017. ISSN 15407489. doi:10.1016/j.proci.2016.08.078.
- [31] E. T. Kho, E. Lovell, R. J. Wong, J. Scott, and R. Amal. Manipulating ceria-titania binary oxide features and their impact as nickel catalyst supports for low temperature steam reforming of methane. *Appl. Catal., A*, 530:111–124, 2017. ISSN 0926860X. doi:10.1016/j.apcata.2016.11.019.

- [32] B.-J. Kim, D. F. Abbott, X. Cheng, E. Fabbri, M. Nachtegaal, F. Bozza, I. E. Castelli, D. Lebedev, R. Schäublin, C. Copéret, T. Graule, N. Marzari, and T. J. Schmidt. Unraveling thermodynamics, stability, and oxygen evolution activity of strontium ruthenium perovskite oxide. *ACS Catal.*, 7(5):3245–3256, 2017. ISSN 2155-5435 2155-5435. doi:10.1021/acscatal.6b03171.
- [33] K. D. Kim, S. Pokhrel, Z. Wang, H. Ling, C. Zhou, Z. Liu, M. Hunger, L. Mädler, and J. Huang. Tailoring high-performance Pd catalysts for chemoselective hydrogenation reactions via optimizing the parameters of the double-flame spray pyrolysis. *ACS Catal.*, 6(4):2372–2381, 2016. ISSN 2155-5435 2155-5435. doi:10.1021/acscatal.6b00396.
- [34] S. Kim, T. D. Myles, H. R. Kunz, D. Kwak, Y. Wang, and R. Maric. The effect of binder content on the performance of a high temperature polymer electrolyte membrane fuel cell produced with reactive spray deposition technology. *Electrochim. Acta*, 177:190–200, 2015. ISSN 00134686. doi:10.1016/j.electacta.2015.02.025.
- [35] R. Koirala, R. Buechel, S. E. Pratsinis, and A. Baiker. Silica is preferred over various single and mixed oxides as support for CO₂-assisted cobalt-catalyzed oxidative dehydrogenation of ethane. *Appl. Catal., A*, 527:96–108, 2016. ISSN 0926860X. doi:10.1016/j.apcata.2016.08.032.
- [36] R. Koirala, S. E. Pratsinis, and A. Baiker. Synthesis of catalytic materials in flames: opportunities and challenges. *Chem. Soc. Rev.*, 45(11):3053–3068, 2016. ISSN 1460-4744 (Electronic) 0306-0012 (Linking). doi:10.1039/c5cs00011d.
- [37] G. Kühner and M. Voll. Manufacture of carbon black. In J.-B. Donnet, editor, *Carbon Black: Science and Technology*, pages 1–66. Marcel Dekker, Inc., New York, 2nd edition, 1993.
- [38] S. Lee, K. Schneider, J. Schumann, A. K. Mogalicherla, P. Pfeifer, and R. Dittmeyer. Effect of metal precursor on Cu/ZnO/Al₂O₃ synthesized by flame spray pyrolysis for direct DME production. *Chem. Eng. Sci.*, 138:194–202, 2015. ISSN 00092509. doi:10.1016/j.ces.2015.08.021.
- [39] S. Li, Y. Ren, P. Biswas, and S. D. Tse. Flame aerosol synthesis of nanostructured materials and functional devices: Processing, modeling, and diagnostics. *Prog. Energy Combust. Sci.*, 55:1–59, 2016. ISSN 03601285. doi:10.1016/j.pecs.2016.04.002.
- [40] G. Liu, J. Hall, N. Nasiri, T. Gengenbach, L. Spiccia, M. H. Cheah, and A. Tricoli. Scalable synthesis of efficient water oxidation catalysts: Insights into the activity of flame-made manganese oxide nanocrystals. *ChemSusChem*, 8(24):4162–4171, 2015. ISSN 1864-564X (Electronic) 1864-5631 (Linking). doi:10.1002/cssc.201500704.
- [41] Y. Liu, J. Huang, Y. Gong, X. Xu, and H. Li. Liquid flame spray fabrication of WO₃-reduced graphene oxide nanocomposites for enhanced O₃-sensing performances. *Ceram. Int.*, 43(16):13185–13192, 2017. ISSN 02728842. doi:10.1016/j.ceramint.2017.07.012.

- [42] E. C. Lovell, J. Horlyck, J. Scott, and R. Amal. Flame spray pyrolysis-designed silica/ceria-zirconia supports for the carbon dioxide reforming of methane. *Appl. Catal., A*, 546:47–57, 2017. ISSN 0926860X. doi:10.1016/j.apcata.2017.08.002.
- [43] M. Y. Manuputty, J. Akroyd, S. Mosbach, and M. Kraft. Modelling TiO₂ formation in a stagnation flame using method of moments with interpolative closure. *Combust. Flame*, 178:135–147, 2017. ISSN 00102180. doi:10.1016/j.combustflame.2017.01.005.
- [44] W. Merchan-Merchan, A. V. Saveliev, L. Kennedy, and W. C. Jimenez. Combustion synthesis of carbon nanotubes and related nanostructures. *Prog. Energy Combust. Sci.*, 36(6):696–727, 2010. ISSN 03601285. doi:10.1016/j.pecs.2010.02.005.
- [45] K. A. Michalow-Mauke, Y. Lu, K. Kowalski, T. Graule, M. Nachtegaal, O. Kröcher, and D. Ferri. Flame-made WO₃/CeO_x-TiO₂ catalysts for selective catalytic reduction of NO_x by NH₃. *ACS Catal.*, 5(10):5657–5672, 2015. ISSN 2155-5435 2155-5435. doi:10.1021/acscatal.5b01580.
- [46] F. Pelletier and B. Thiébaud. Improvement of noble metal based photocatalysts by spray pyrolysis processes. *Johnson Matthey Technol. Rev.*, 60(1):39–54, 2016. ISSN 20565135. doi:10.1595/205651315x689829.
- [47] B. Pongthawornsakun, O. Mekasuwandumrong, F. J. C. Santos Aires, R. Büchel, A. Baiker, S. E. Pratsinis, and J. Panpranot. Variability of particle configurations achievable by 2-nozzle flame syntheses of the Au-Pd-TiO₂ system and their catalytic behaviors in the selective hydrogenation of acetylene. *Appl. Catal., A*, 549:1–7, 2018. ISSN 0926860X. doi:10.1016/j.apcata.2017.09.014.
- [48] M. Punginsang, A. Wisitsoraat, C. Sriprachuabwong, D. Phokharatkul, A. Tuantrantont, S. Phanichphant, and C. Liewhiran. Roles of cobalt doping on ethanol-sensing mechanisms of flame-spray-made SnO₂ nanoparticles-electrolytically exfoliated graphene interfaces. *Appl. Surf. Sci.*, 425:351–366, 2017. ISSN 01694332. doi:10.1016/j.apsusc.2017.06.265.
- [49] J. Rebholz, K. Grossmann, D. Pham, S. Pokhrel, L. Madler, U. Weimar, and N. Barsan. Selectivity enhancement by using double-layer MOX-based gas sensors prepared by flame spray pyrolysis (FSP). *Sensors (Basel)*, 16(9):1437, 2016. ISSN 1424-8220 (Electronic) 1424-8220 (Linking). doi:10.3390/s16091437.
- [50] M. Righettoni, A. Tricoli, and S. E. Pratsinis. Thermally stable, silica-doped ε-WO₃ for sensing of acetone in the human breath. *Chem. Mater.*, 22(10):3152–3157, 2010. ISSN 0897-4756 1520-5002. doi:10.1021/cm1001576.
- [51] J. Roller, J. Renner, H. Yu, C. Capuano, T. Kwak, Y. Wang, C. B. Carter, K. Ayers, W. E. Mustain, and R. Maric. Flame-based processing as a practical approach for manufacturing hydrogen evolution electrodes. *J. Power Sources*, 271:366–376, 2014. ISSN 03787753. doi:10.1016/j.jpowsour.2014.08.013.

- [52] J. M. Roller, S. Kim, T. Kwak, H. Yu, and R. Maric. A study on the effect of selected process parameters in a jet diffusion flame for Pt nanoparticle formation. *J. Mater. Sci.*, 52(16):9391–9409, 2017. ISSN 0022-2461 1573-4803. doi:10.1007/s10853-017-1101-y.
- [53] P. Roth. Particle synthesis in flames. *Proc. Combust. Inst.*, 31(2):1773–1788, 2007. ISSN 15407489. doi:10.1016/j.proci.2006.08.118.
- [54] T. Samerjai, D. Channei, C. Khanta, K. Inyawilert, C. Liewhiran, A. Wisitsoraat, D. Phokharatkul, and S. Phanichphant. Flame-spray-made ZnInO alloyed nanoparticles for NO₂ gas sensing. *J. Alloys. Compd.*, 680:711–721, 2016. ISSN 09258388. doi:10.1016/j.jallcom.2016.04.160.
- [55] M. Schubert, S. Pokhrel, A. Thomé, V. Zielasek, T. M. Gesing, F. Roessner, L. Mädler, and M. Bäumer. Highly active Co-Al₂O₃-based catalysts for CO₂ methanation with very low platinum promotion prepared by double flame spray pyrolysis. *Catal. Sci. Technol.*, 6(20):7449–7460, 2016. ISSN 2044-4753 2044-4761. doi:10.1039/c6cy01252c.
- [56] K. Siritworarat, V. Deerattrakul, P. Dittanet, and P. Kongkachuichay. Production of methanol from carbon dioxide using palladium-copper-zinc loaded on MCM-41: Comparison of catalysts synthesized from flame spray pyrolysis and sol-gel method using silica source from rice husk ash. *J. Cleaner Prod.*, 142:1234–1243, 2017. ISSN 09596526. doi:10.1016/j.jclepro.2016.07.099.
- [57] R. Strobel and S. E. Pratsinis. Flame aerosol synthesis of smart nanostructured materials. *J. Mater. Chem.*, 17(45):4743, 2007. ISSN 0959-9428 1364-5501. doi:10.1039/b711652g.
- [58] J. Sukunta, A. Wisitsoraat, A. Tuantranont, S. Phanichphant, and C. Liewhiran. Highly-sensitive H₂S sensors based on flame-made V-substituted SnO₂ sensing films. *Sens. Actuators, B*, 242:1095–1107, 2017. ISSN 09254005. doi:10.1016/j.snb.2016.09.140.
- [59] N. Tammanoon, A. Wisitsoraat, C. Sriprachuabwong, D. Phokharatkul, A. Tuantranont, S. Phanichphant, and C. Liewhiran. Ultrasensitive NO₂ sensor based on ohmic metal-semiconductor interfaces of electrolytically exfoliated graphene/flame-spray-made SnO₂ nanoparticles composite operating at low temperatures. *ACS Appl. Mater. Interfaces*, 7(43):24338–24352, 2015. ISSN 1944-8252 (Electronic) 1944-8244 (Linking). doi:10.1021/acsami.5b09067.
- [60] I. Tantis, M. V. Dozzi, L. G. Bettini, G. L. Chiarello, V. Dracopoulos, E. Selli, and P. Lianos. Highly functional titania nanoparticles produced by flame spray pyrolysis. photoelectrochemical and solar cell applications. *Appl. Catal., B*, 182:369–374, 2016. ISSN 09263373. doi:10.1016/j.apcatb.2015.09.040.
- [61] G. D. Ulrich. Flame synthesis of fine particles. *Chem. Eng. News*, 62(32):22–29, 1984. ISSN 0009-2347. doi:10.1021/cen-v062n032.p022.

- [62] E. Wagner and H. Brünner. Aerosil, Herstellung, Eigenschaften und Verhalten in organischen Flüssigkeiten. *Angew. Chem.*, 72(19-20):744–750, 1960. ISSN 00448249 15213757. doi:10.1002/ange.19600721907.
- [63] H. Wang. Formation of nascent soot and other condensed-phase materials in flames. *Proc. Combust. Inst.*, 33(1):41–67, 2011. ISSN 15407489. doi:10.1016/j.proci.2010.09.009.
- [64] N. Wang, S. Li, Y. Zong, and Q. Yao. Sintering inhibition of flame-made Pd/CeO₂ nanocatalyst for low-temperature methane combustion. *J. Aerosol Sci.*, 105:64–72, 2017. ISSN 00218502. doi:10.1016/j.jaerosci.2016.11.017.
- [65] N. Wang, S. Li, Y. Zong, Q. Yao, and Y. Zhang. Flame synthesis of novel ternary nanocatalysts Pd/CeO₂-TiO₂ with promotional low-temperature catalytic oxidation properties. *Proc. Combust. Inst.*, 36(1):1029–1036, 2017. ISSN 15407489. doi:10.1016/j.proci.2016.08.060.
- [66] S. Wang, Z. Lan, and Y. Huang. Flame aerosol synthesis of tungsten trioxide powder: Particle morphology control and photodegradation activity under visible light irradiation. *Powder Technol.*, 294:259–265, 2016. ISSN 00325910. doi:10.1016/j.powtec.2016.02.043.
- [67] Z. Wang, J. Huang, R. Amal, and Y. Jiang. Solid-state NMR study of photocatalytic oxidation of acetaldehyde over the flame-made F-TiO₂ catalyst. *Appl. Catal., B*, 223:16–21, 2018. ISSN 09263373. doi:10.1016/j.apcatb.2017.04.011.
- [68] L. White and G. Duffy. Staff-industry collaborative report vapor-phase production of colloidal silica. *Ind. Eng. Chem.*, 51(3):232–238, 1959. ISSN 0019-7866 1541-5724. doi:10.1021/ie51394a019.
- [69] Z. Xiong, Z. Lei, Z. Xu, X. Chen, B. Gong, Y. Zhao, H. Zhao, J. Zhang, and C. Zheng. Flame spray pyrolysis synthesized ZnO/CeO₂ nanocomposites for enhanced CO₂ photocatalytic reduction under UV-Vis light irradiation. *J. CO₂ Util.*, 18:53–61, 2017. ISSN 22129820. doi:10.1016/j.jcou.2017.01.013.
- [70] Y. Xu, M. Kraft, and R. Xu. Metal-free carbonaceous electrocatalysts and photocatalysts for water splitting. *Chem. Soc. Rev.*, 45(11):3039–3052, 2016. ISSN 1460-4744 (Electronic) 0306-0012 (Linking). doi:10.1039/c5cs00729a.
- [71] J. Yu, Z. Zhang, F. Dallmann, J. Zhang, D. Miao, H. Xu, A. Goldbach, and R. Dittmeyer. Facile synthesis of highly active Rh/Al₂O₃ steam reforming catalysts with preformed support by flame spray pyrolysis. *Appl. Catal., B*, 198:171–179, 2016. ISSN 09263373. doi:10.1016/j.apcatb.2016.05.050.
- [72] T. Zhou, Y. Du, S. Yin, X. Tian, H. Yang, X. Wang, B. Liu, H. Zheng, S. Qiao, and R. Xu. Nitrogen-doped cobalt phosphate@nanocarbon hybrids for efficient electrocatalytic oxygen reduction. *Energy Environ. Sci.*, 9(8):2563–2570, 2016. ISSN 1754-5692 1754-5706. doi:10.1039/c6ee01297c.

- [73] T. Zhou, Y. Du, D. Wang, S. Yin, W. Tu, Z. Chen, A. Borgna, and R. Xu. Phosphonate-based metal-organic framework derived Co-P-C hybrid as an efficient electrocatalyst for oxygen evolution reaction. *ACS Catal.*, 7(9):6000–6007, 2017. ISSN 2155-5435 2155-5435. doi:10.1021/acscatal.7b00937.
- [74] Y. Zong, S. Li, F. Niu, and Q. Yao. Direct synthesis of supported palladium catalysts for methane combustion by stagnation swirl flame. *Proc. Combust. Inst.*, 35(2): 2249–2257, 2015. ISSN 15407489. doi:10.1016/j.proci.2014.06.114.